J. Fluid Mech. (2001), *vol.* 435, *pp.* 377–396. Printed in the United Kingdom

Virtual origin correction for lazy turbulent plumes

By G. R. HUNT† AND N. G. KAYE

Department of Applied Mathematics and Theoretical Physics,
Silver Street, Cambridge CB3 9EW, UK

(Received 10 September 1997 and in revised form 26 June 2000)

The location of the asymptotic virtual origin of positively buoyant turbulent plumes with a deficit of initial momentum flux when compared with equivalent pure plumes is investigated. These *lazy* plumes are generated by continuous steady releases of momentum, buoyancy and volume into a quiescent uniform environment from horizontal sources (at $z = 0$) of finite area, and are shown to be equivalent to the far-field flow above point source pure plumes, of buoyancy only, rising from the asymptotic virtual source located below the actual source at $z = -z_{avs}$.

An analytical expression for the location of the asymptotic virtual source relative to the actual source of the lazy plume is developed. The plume conservation equations are solved for the volume flow rate, and the position of the asymptotic virtual origin is deduced from the scaling for the volume flow rate at large distances from the source.

The displacement z_{avs} of the asymptotic virtual origin from the actual origin scales on the source diameter and is a function of the source parameter $\Gamma \propto \hat{Q}_0^2\hat{F}_0/\hat{M}_0^{5/2}$ which is a measure of the relative importance of the initial fluxes of buoyancy $\hat{F}_0$, momentum $\hat{M}_0$, and volume $\hat{Q}_0$ in the plume. The virtual origin correction developed is valid for $\Gamma > 1/2$ and is therefore applicable to lazy plumes for which $\Gamma > 1$, pure plumes for which $\Gamma = 1$, and forced plumes in the range $1/2 < \Gamma < 1$. The dimensionless correction z^*_{avs} decreases as Γ increases, and for $\Gamma \gg 1$, $z^*_{avs} \to 0.853\Gamma^{-1/5}$. Comparisons made between the predicted location of the asymptotic virtual origin and the location inferred from measurements of lazy saline plumes in the laboratory show close agreement.

1. Introduction

Turbulent plumes are encountered in nature and in industry and on a variety of different scales – from releases of hot ash during volcanic eruptions to the flow above electronic components. Numerous field and laboratory studies have been conducted over the years in order to examine the flow in and the flow induced by plumes, e.g. Morton (1959*b*) measures the rise heights of plumes from industrial chimneys in order to predict the spread of pollution in the atmosphere. The time-averaged behaviour of turbulent plumes has been described theoretically by Morton, Taylor & Turner (1956, referred to hereinafter as MTT), who derived similarity solutions expressing the mean quantities in the plume as functions of the buoyancy flux and vertical distance above the source. MTT model entrainment into the plume by relating the

† Present address: Department of Civil and Environmental Engineering, Imperial College of Science Technology and Medicine, Imperial College Road, London SW7 2BU, UK.

horizontal entrainment velocity to the vertical velocity in the plume at that height via a (constant) entrainment coefficient. This approach has been widely applied to model a variety of flows involving plumes. Much of this research is summarized by Turner (1986) and List (1982). An improved description of the entrainment process in which the entrainment is characterized in terms of the local fluxes in the plume is given by Kotsovinos & List (1977).

In order to predict accurately the flow in a turbulent plume, it is essential to model the source conditions correctly. The classical plume theory developed by MTT assumes an idealized plume source, that is, a point source of buoyancy flux with zero initial fluxes of volume and momentum. For clarity, source conditions will be represented hereinafter using the notation (F_0, M_0, Q_0), where the quantities $F_0 = 2\hat{F}_0/\pi$, $M_0 = 2\hat{M}_0/\pi$ and $Q_0 = \hat{Q}_0/\pi$ are proportional to the actual initial fluxes of buoyancy $\hat{F}_0$, momentum $\hat{M}_0$ and volume $\hat{Q}_0$, respectively. For an axisymmetric plume the actual fluxes are defined as

$$\hat{F} = 2\pi \int_0^\infty wg'r \, \mathrm{d}r, \quad \hat{M} = 2\pi \int_0^\infty w^2 r \, \mathrm{d}r, \quad \hat{Q} = 2\pi \int_0^\infty wr \, \mathrm{d}r, \tag{1}$$

where r denotes the radial or cross-plume coordinate, z the vertical coordinate, $w(r, z)$ the vertical velocity and $g'(r, z) = g(\rho_e - \rho)/\rho_0$ the reduced gravity; ρ, ρ_e and ρ_0 denote the density of the plume, the environment and a reference density, respectively. In most practical situations, plumes issue from sources of finite area, e.g. smoke plumes from chimneys or plumes generated in the laboratory (§ 3), rather than idealized point sources assumed in the plume theory. A separate calculation, or correction, is then needed to relate the position of the actual area source we wish to model to a point source located at a virtual origin before the theory can be confidently used to make predictions.

A number of authors have investigated this problem and their virtual origin corrections may be roughly grouped into four different categories: (i) corrections based on empirical measurements; (ii) a 'conical' source correction; (iii) a jet-length based correction; and (iv) a source correction based on the initial properties $\hat{F}_0$, $\hat{M}_0$ and $\hat{Q}_0$ of the plume.

1.1. *Corrections based on empirical measurements*

It is often possible to infer the location of the virtual origin by analysis of experimental results (MTT; Turner 1966). For example, by graphically illustrating scaled quantities in the plume as a function of the vertical distance z from the actual source, the virtual origin may be determined simply by extrapolating a fit to the data for $z < 0$. An estimate of the location of the virtual origin is given by the point of intercept of the extrapolated data with the z-axis.

Another example of the use of empirical measurements to determine the location of the virtual origin is given by Baines & Turner (1969) who theoretically predict and make measurements of the position z_0 of the first 'front' produced by an axisymmetric plume in a filling box as a function of time t. Baines & Turner (1969) plot their experimental observations in a form suggested by their theory, namely $z_0^{-2/3}$ against t, and correct the measured height z_0 iteratively by adding a constant length z_v until the modified height $(z_0 + z_v)^{-2/3}$ scales correctly (in this case linearly) with time. The value of z_v which provided the correct scaling was taken as the origin correction. This technique was found to provide a sensitive estimate of the position of the virtual origin.

In an appendix to their paper, George, Alpert & Tamanini (1977) describe a similar technique to determine the virtual origin from plume data. They note that

the similarity solutions (Batchelor 1954) for the time-averaged vertical velocity w and reduced gravity g' in the plume, namely,

$$w \propto (z - z_v)^{-1/3}, \quad g' \propto (z - z_v)^{-5/3}, \tag{2a,b}$$

may be written in the form

$$w^3 z = w^3 z_v + k_1, \quad g'^{3/5} z = g'^{3/5} z_v + k_2, \tag{3a,b}$$

where k_1 and k_2 are constants. Hence, the gradient of the plot of $w^3 z$ *vs.* w^3 or $g'^{3/5} z$ *vs.* $g'^{3/5}$ yields the location $z = -z_v$ of the virtual origin. George *et al.* (1977) suggest that if fractional errors in the measurements of g' and w are comparable, the position of the origin inferred from buoyancy measurements, rather than from vertical velocity, should yield a more reliable result as errors in g' are raised only to the power of 3/5 (equation (3*b*)) whereas errors in w are cubed (equation (3*a*)).

1.2. *'Conical' correction*

Schmidt (1941) observed that plumes of hot air rising from small sources into a quiescent environment tend to be confined within conical regions when the flow is turbulent. This early observation has been verified by numerous subsequent field and laboratory studies. MTT present a simple method for determining the virtual origin of a buoyant plume based on their classical plume theory and the plume's conical shape. They determine the location of the virtual source by treating a plume from a finite area source as a circular cone. The bounding surface for the cone is chosen, somewhat arbitrarily, by introducing an 'effective' plume radius which is defined as the radius to points at which the mean amplitude of the profile (of velocity or buoyancy) has decreased to, say, c% of the peak axial value, where c is small. The effective radius may be deduced either from experimental measurement or predicted by plume theory. Once c has been specified, the location of the virtual origin is determined simply by tracing the cone back to its apex. This technique is depicted in figure 1 where it can be seen that the displacement z_v of the virtual origin from the actual source decreases as c decreases.

Assuming Gaussian profiles† of the form $\exp(-r^2/b^2)$ for mean vertical velocity and buoyancy profiles, the diameter D of the source in terms of the c% plume width is given by $D = 2b\sqrt{-\ln(c)}$. The radius b of the plume as a function of the vertical distance z from the source is described by $b/(z + z_v) = 6\alpha/5$ (see MTT) and, hence, the virtual source is located behind the actual source and at $z = -z_v$, where

$$\frac{z_v}{D} = \frac{5}{12\alpha\sqrt{-\ln(c)}}. \tag{4}$$

† Detailed measurements of mean flow quantities by Shabbir & George (1994) and Papanicolaou & List (1988) indicate that the mean profiles of vertical velocity and buoyancy in turbulent plumes are self-similar after 5 or 6 jet lengths (see §1.3) from the source and are well described by Gaussian profiles of the form $A\exp(B\eta^2)$, where $\eta = r/z$. There is, however, some uncertainty in the literature regarding the most appropriate value for the coefficient A and the exponent B. Measurements by George *et al.* (1977) suggest that the mean vertical velocity profile is wider than the buoyancy profile – a result supported by the measurements of Nakagome & Hirita (1977) and Shabbir & George (1994). However, Rouse, Yih & Humphreys (1952) and Papanicolaou & List (1988) conclude the opposite result. George *et al.* (1977) found the numerical values deduced from the early experiments of Rouse *et al.* (1952) to be in error as their measurements did not account for the turbulent transport of buoyancy which contributes roughly 15% to the total buoyancy transport. In light of these uncertainties, and for simplicity, we shall assume in §2 that the vertical velocity and buoyancy profiles have equal widths.

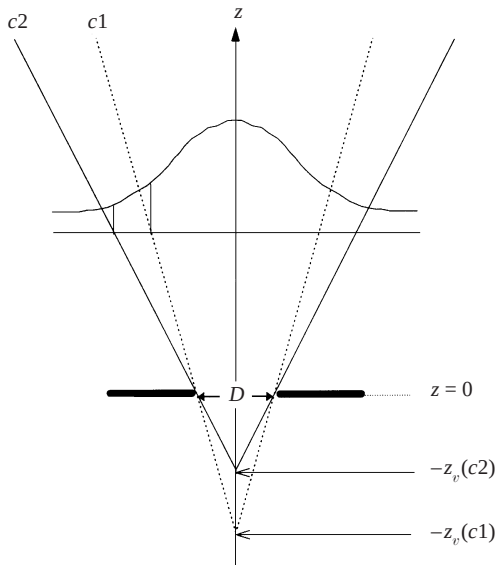

FIGURE 1. The 'conical' correction technique for predicting the location of the virtual origin of a plume. The actual source, of diameter D, is at $z = 0$ and the virtual source is at $z = -z_v$. The virtual origin is shown for two values of c with $c1 > c2$.

This correction assumes the flow in the plume is fully developed, i.e. of self-similar Gaussian profile, at the actual origin. Although self-similarity of profiles is evident sufficiently far from the source (Shabbir & George 1994; Papanicolaou & List 1988), profiles at the source are unlikely to be self-similar or Gaussian. Comparisons presented by MTT between the experimentally determined displacement of the virtual origin and the results predicted by (4) for $c = 1\%$ and $c = 1/10\%$ show reasonable agreement and highlight the sensitivity of the prediction to the choice of c.

The location of the virtual origin may also be determined from the line defined by the plume envelope. This is simple to determine from a photo or video still by drawing a line along the edges of the turbulent region; the total angle θ enclosed is approximately 18°–20°. This provides the following geometrical estimate for the distance the virtual source lies behind the actual source:

$$\frac{z_v}{D} = \frac{1}{2\tan(\frac{1}{2}\theta)}. \tag{5}$$

1.3. *Jet-length-based correction*

Morton (1959*a*) shows that the flow above a point source forced plume $(F_0, M_0, 0)$ of buoyancy and momentum only, develops into a pure plume at a vertical distance above the source which scales on the momentum jet length L_m, where

$$L_m = 2^{-3/2}\alpha^{-1/2}\frac{M_0^{3/4}}{F_0^{1/2}}, \tag{6}$$

and α denotes the plume entrainment coefficient (see MTT) appropriate for Gaussian profiles. (A plume is 'pure' if the volume, momentum and buoyancy fluxes satisfy the ratio $5Q^2(z)F/4\alpha M^{5/2}(z) = 1$. This constraint may be satisfied at the source (see § 1.4), in which case the source emits a pure (or simple) plume, otherwise the ratio of the local fluxes tends towards unity as the flow rises above the source.) The lengthscale L_m represents the vertical distance over which the forced plume is driven primarily

by the initial momentum flux, i.e. where the flow is more jet-like than plume-like. For $z > L_m$, the momentum flux generated by the action of the buoyancy forces dominates the motion. The significance of L_m in characterizing the vertical evolution of the flow from a buoyant source of non-zero initial momentum flux is discussed in detail by Baker, George & Taulbee (1980).

By considering the solution of the plume conservation equations subject to the boundary conditions $F = F_0$, $M = M_0$ and $Q = 0$ at $z = 0$, Morton (1959*a*) deduces that the flow above the point source pure plume $(F_0, 0, 0)$ positioned at $z = -1.057L_m$ exhibits the behaviour of the flow from the source $(F_0, M_0, 0)$ to within 1% for $z/L_m \geqslant 5$. In other words, the virtual source is located a distance

$$\frac{z_{avs}}{L_m} = -1.057 \tag{7}$$

behind the given source, see Appendix A. This correction is referred to as an asymptotic virtual source as the point source pure plume rising from $z = z_{avs}$ tends towards the behaviour of the forced plume released from $z = 0$ only for sufficiently large distances above the original source, in this case $z/L_m \geqslant 5$.

1.4. *Source correction based on initial* (F_0, M_0, Q_0)

Morton (1959*a*) also presents a theoretical technique for determining the location of the virtual origin of a plume from a more general extended, or area, source of buoyancy, momentum and volume. Morton shows that it is always possible to relate the flow above a general source (F_0, M_0, Q_0) at $z = 0$ to an equivalent point source forced plume $(F_0, \gamma M_0, 0)$, of buoyancy and momentum only, with modified strength γM_0 and modified position $z = z_v$. The point source plume $(F_0, \gamma M_0, 0)$ at $z = z_v$ is forced to satisfy the same equations as the plume from the general source, and the momentum and volume fluxes in the two plumes are matched at $z = 0$ in order to determine the location z_v and strength γM_0 of the modified plume. A parametric solution for a plume issuing from the source (F_0, M_0, Q_0) is given in terms of the momentum flux and it is shown that the two plumes will be identical above the actual source if the origin of the point source $(F_0, \gamma M_0, 0)$ is a distance

$$\frac{z_v}{L_m} = -10^{1/2}|\gamma|^{3/2}\operatorname{sgn} F_0 \int_{\operatorname{sgn}\gamma}^{1/|\gamma|} |T^5 - \operatorname{sgn}\gamma|^{-1/2} T^3 \,\mathrm{d}T, \tag{8}$$

from the actual source, where the modification factor

$$\gamma^5 = 1 - \Gamma, \tag{9}$$

depends on the source parameter

$$\Gamma = \frac{5Q_0^2 F_0}{4\alpha M_0^{5/2}}. \tag{10}$$

Both positive and negatively buoyant sources are considered by Morton and $\operatorname{sgn} F_0 = \pm 1$ accordingly. Depending on the source conditions, as set by Γ, Morton's solution, (8)–(10), predicts modified plumes with either positive or negative initial momentum fluxes and $\operatorname{sgn}\gamma = \pm 1$ according to whether $\gamma > 0$ or $\gamma < 0$, respectively. In contrast to the asymptotic origin correction discussed in § 1.3, the correction (8) is exact as the flow above the point source is identical above $z = 0$ to the flow above the original extended source.

The source parameter Γ is the inverse square of a source Froude number, see

Baines (1983), and provides a measure of the relative importance of the initial fluxes of buoyancy, momentum and volume in the plume. Morton (1959*a*) categorizes buoyant plumes in terms of Γ, defining forced plumes, i.e. those for which the initial momentum flux is greater than that of an equivalent pure plume of the same initial buoyancy flux, for $0 < \Gamma < 1$; pure plumes as those with source conditions giving $\Gamma = 1$; and lazy plumes, i.e. those in which the initial momentum flux is less than that of a pure plume of the same initial buoyancy flux, for $\Gamma > 1$.

Morton's (1959*a*) theoretical description (8) provides a practical solution for forced buoyant plumes ($0 < \Gamma < 1$) and pure plumes ($\Gamma = 1$), however, for lazy plumes ($\Gamma > 1$) it is physically unrealistic as it requires $\gamma < 0$, i.e. for the initial momentum flux of the virtual point source to be directed downwards thereby resulting in flow in both downward and upward directions near the source. The physical interpretation of the solution for $\Gamma > 1$ is that forcing buoyant fluid downwards from a suitably located point source allows the momentum flux generated by the action of the buoyancy forces to cancel out the initial momentum flux and to subsequently produce a broad ascending positively buoyant plume of appreciable volume flux but low ascent velocity, i.e. a lazy plume, at $z = 0$.

The work of Morton (1959*a*) is extended by Morton & Middleton (1973) who illustrate in a graphical form the location of the virtual origin, scaled on the jet length, for plumes with source conditions corresponding to $\Gamma < 5$. These scale diagrams indicate that for $\Gamma \gtrsim 1.25$ the initial momentum of the modified source is again directed downwards but from a point located above the physical source (see solid curve labelled x_{vs} in figure 2 of Morton & Middleton 1973).

The methods of Morton (1959*a*) as outlined in § 1.4 and § 1.3 can be combined to give a two-step procedure for relating the flow above a general extended source (F_0, M_0, Q_0) at $z = 0$ to the flow from an asymptotic virtual point source $(F_0, 0, 0)$ at $z = z_{avs}$. The first step (§ 1.4) involves replacing the extended source (F_0, M_0, Q_0) with a virtual point source forced plume of modified strength $(F_0, \gamma M_0, 0)$ located at $z = z_v$. The sign of z_v depends upon the source parameter Γ and may be positive or negative. The second step (§ 1.3) relates the flow above this modified source to a pure buoyancy source $(F_0, 0, 0)$ at $z = z_{avs}$. Combining the two steps, the far-field flow produced by the general source (F_0, M_0, Q_0) at $z = 0$ may be related to the flow above the point buoyancy source $(F_0, 0, 0)$ at the virtual origin $z = z_v + z_{avs}$. The full 'two-step' solution is not written down explicitly by Morton (1959*a*), although Morton & Middleton (1973, figure 2, dashed curve labelled x_{avs}) plot the two-step correction as a function of Γ. For a buoyant area source with positive initial momentum flux the two-step correction may be shown to take the following forms:

(*a*) *Pure plumes* ($\Gamma = 1$) from area sources may be related to the virtual source $(F_0, 0, 0)$ in a single step as, from (9), the solution requires $\gamma = 0$. The correction is exact and the virtual source $(F_0, 0, 0)$ is located at

$$\frac{z_v}{L_m} = -2^{3/2}5^{1/2}3^{-1} \approx -2.108. \tag{11}$$

(*b*) *Forced plumes* ($0 < \Gamma < 1$) require both steps. The momentum flux of the modified source is positive as $\gamma = (1 - \Gamma)^{1/5} > 0$ and the total magnitude of the two-step correction is

$$\frac{z_v + z_{avs}}{L_m} = \underbrace{-10^{1/2} \int_\gamma^1 v^3 (v^5 - \gamma^5)^{-1/2} \, \mathrm{d}v}_{z_v/L_m} \underbrace{- 10^{-1/2}\gamma^{3/2}(\tfrac{2}{3} + \delta_{fp})}_{z_{avs}/L_m}, \tag{12a}$$

where

$$\delta_{fp} = \sum_{n=1}^{\infty} \left(\frac{1}{2^{n-1} n!(3-10n)} \prod_{j=1}^{n} (1 + 2[j-1]) \right). \tag{12b}$$

Series (12*b*) sums to $\delta_{fp} = -0.3324$ and thus, from (12*a*)

$$\frac{z_{avs}}{L_m} = -1.057\gamma^{3/2}, \tag{12c}$$

which is accurate to within 1% for $z/L_m > 6\gamma^{3/2}$.

(*c*) *Lazy plumes* ($\Gamma > 1$) also require a two-step correction. The modified source has negative momentum flux as $\gamma = -(\Gamma - 1)^{1/5} < 0$ and the two-step procedure yields

$$\frac{z_v + z_{avs}}{L_m} = \underbrace{-10^{1/2} \int_{-|\gamma|}^{1} v^3 (v^5 + |\gamma|^5)^{-1/2} \mathrm{d}v}_{z_v/L_m} \underbrace{- |\gamma|^{3/2} 3.253}_{z_{avs}/L_m}, \tag{13}$$

where z_{avs} is accurate to within 1% for $z/L_m > 4|\gamma|^{3/2}$.

In (*a*)–(*c*) above, the correction z_v is exact and z_{avs} appropriate at only large distances from the actual source, thus corrections (12*a*) and (13) represent the location of the pure buoyancy source $(F_0, 0, 0)$ from which the far-field behaviour of the extended source (F_0, M_0, Q_0) appears to tend and are thus asymptotic corrections.

Caulfield (1991) presents an alternative classification scheme based on the parameter $C_c = 1 - 1/\Gamma$ and determines origin corrections for general extended plume sources. By manipulating MTT's plume conservation equations, Caulfield expresses $Q(z)$ as a function of Q_0, F_0 and C_c, and solves the resulting single equation numerically. Caulfield (1991) deduces the asymptotic virtual origin for $-\infty < C_c \leqslant 1$ (or, equivalently, $0 < \Gamma < \infty$) by tracing the evolution of the plume until it approaches the pure plume solution of MTT. Caulfield also determines the source conditions for which lazy plumes initially contract, or 'neck', as they rise above the source. Following Caulfield we note that contraction occurs directly above the source if the rate of change of the plume radius b with height satisfies

$$\left.\frac{\mathrm{d}b}{\mathrm{d}z}\right|_{z=0} = 2\alpha - \frac{4\alpha\Gamma}{5} < 0, \tag{14}$$

i.e. providing $\Gamma > 2.5$. By analysis of the plume undergoing contraction, Caulfield (1991) deduces that a plume can accelerate above the source without contracting, but not vice versa, as acceleration occurs directly above the source if

$$\left.\frac{\mathrm{d}w_m}{\mathrm{d}z}\right|_{z=0} = \frac{2g'_m}{w_m} - \left.\frac{2\alpha w_m}{b}\right|_{z=0} > 0, \tag{15}$$

i.e. providing $\Gamma = (5/4\alpha)(bg'_m/w_m^2) > 1.25$, where w_m and g'_m denote the axial vertical velocity and reduced gravity, respectively. The analysis of Caulfield addresses plumes with monotonic and non-monotonic mixing behaviours, for the latter case see also Caulfield & Woods (1995).

In this paper we present a single-step method for determining the displacement of the asymptotic virtual source $(F_0, 0, 0)$ from the actual source (F_0, M_0, Q_0) of a lazy plume. The approach we adopt is similar to that presented by Morton (1959*a*), however, we show for lazy plumes that it is possible to describe analytically their far-field behaviour in terms of a pure point source $(F_0, 0, 0)$, of buoyancy only, at the asymptotic virtual origin z_{avs} located behind the given source. Our analysis provides a

physically realistic solution as it does not involve directing buoyant fluid downwards with negative initial momentum flux and so avoids a region of counter-flowing fluid near the source. We demonstrate that the appropriate lengthscale for the adjustment of a lazy plume to a pure plume is the source radius, and an explicit formulation is given for calculating the asymptotic virtual origin for source conditions corresponding to $\Gamma > 1/2$. Experiments to measure the volume flow rate above lazy plumes are conducted to compare with the theory.

2. Asymptotic virtual origin location for a lazy plume source

Assuming Gaussian profiles for vertical velocity and buoyancy and an unstratified quiescent environment, the plume equations for conservation of volume, momentum and buoyancy, under the Boussinesq approximation, may be written in the form

$$\frac{\mathrm{d}Q}{\mathrm{d}z} = 2\alpha M^{1/2}, \tag{16}$$

$$\frac{\mathrm{d}M}{\mathrm{d}z} = 2\frac{QF}{M}, \tag{17}$$

$$\frac{\mathrm{d}F}{\mathrm{d}z} = 0, \tag{18}$$

respectively, see MTT, where $Q = b^2 w_m$, $M = b^2 w_m^2$ and $F = b^2 w_m g'_m$. Equation (18) expresses that the buoyancy flux is conserved in an unstratified environment, hence, $F = \text{const} = F_0$. For a general area source, the source conditions are

$$Q = Q_0, \quad M = M_0, \quad F = F_0 \quad \text{at } z = 0. \tag{19}$$

Equation (16) may be rewritten as

$$\int_0^z \mathrm{d}z = \int_{Q_0}^{Q} \frac{\mathrm{d}Q}{2\alpha M^{1/2}}, \tag{20}$$

and, hence, from (17) and (20), we may eliminate z and write

$$\int_{M_0}^{M} M^{3/2}\,\mathrm{d}M = \frac{F}{\alpha}\int_{Q_0}^{Q} Q\,\mathrm{d}Q. \tag{21}$$

Integrating (21) yields

$$M^{5/2} - M_0^{5/2} = \frac{5F}{4\alpha}(Q^2 - Q_0^2). \tag{22}$$

Scaling the variables in the plume on the source conditions, we introduce the non-dimensional quantities

$$m = \frac{M}{M_0}, \quad q = \frac{Q}{Q_0}, \quad f = \frac{F}{F_0}, \tag{23}$$

and, hence, (22) reduces to

$$m^{5/2} = \Gamma(q^2 - 1) + 1, \tag{24}$$

where Γ, the source parameter, is defined in (10). In terms of the actual physical fluxes

$$\Gamma = \frac{5}{2^{7/2}\alpha\pi^{1/2}}\left(\frac{\hat{Q}_0^2\hat{F}_0}{\hat{M}_0^{5/2}}\right), \tag{25}$$

and rewriting (25) in terms of the source area $A\,(=\frac{1}{4}\pi D^2)$ and initial reduced gravity $g_0' = g\Delta\rho_0/\rho_0$, where $\Delta\rho_0$ is the initial density contrast, we obtain

$$\Gamma \sim \frac{A^{5/2} g_0'}{\hat{Q}_0^2}. \tag{26}$$

From (26), we note that Γ can be increased by increasing A, increasing g_0', or decreasing $\hat{Q}_0$, in each case with all other quantities fixed. Thus, highly buoyant slow releases from large area sources give lazy plumes. For the circular sources of interest here, $\Gamma \sim D^5$ and, hence, Γ rapidly increases and the plume becomes increasingly lazy as the area of the source is increased. Substituting (24) into the non-dimensional form of (20) we have

$$z^* = \frac{3}{5}\int_1^q \frac{\mathrm{d}q}{m^{1/2}}, \tag{27}$$

where the vertical coordinate z is scaled on the initial pure plume radius $b_0 = Q_0/M_0^{1/2}(\sim D)$ such that the dimensionless vertical coordinate

$$z^* = \frac{z}{\dfrac{5}{6\alpha}\left(\dfrac{Q_0}{M_0^{1/2}}\right)}. \tag{28}$$

Combining (24) and (27) leads to

$$\Gamma^{1/5} z^* = \frac{3}{5}\int_1^q (q^2 - \phi)^{-1/5}\,\mathrm{d}q, \tag{29}$$

where

$$\phi = \frac{(\Gamma - 1)}{\Gamma}. \tag{30}$$

Expanding the integrand in (29) in terms of ϕ/q^2 we obtain

$$\Gamma^{1/5} z^* = \frac{3}{5}\int_1^q q^{-2/5}\left(1 + \frac{1}{5}\frac{\phi}{q^2} + \frac{1}{5}\frac{6}{5}\frac{\phi^2}{q^4}\frac{1}{2!} + \frac{1}{5}\frac{6}{5}\frac{11}{5}\frac{\phi^3}{q^6}\frac{1}{3!} + \cdots\right)\mathrm{d}q, \tag{31}$$

for $|\phi/q^2| < 1$; this constraint is satisfied over the entire range of integration for $\Gamma > 0.5$. Integrating (31) term by term gives

$$\Gamma^{1/5} z^* = \tfrac{3}{5}(\tfrac{5}{3}q^{3/5} + O(q^{-7/5}) - (\tfrac{5}{3} - \tfrac{1}{7}\phi - \tfrac{3}{85}\phi^2 - \cdots)), \tag{32}$$

which, when rearranged, gives the standard volume flux scaling in the limit of large q, namely

$$q = \Gamma^{1/3}(z^* + z^*_{avs})^{5/3}. \tag{33}$$

The dimensionless asymptotic virtual origin is thus located at $z^* = -z^*_{avs}$, where

$$z^*_{avs} = \Gamma^{-1/5}(1 - \delta), \tag{34}$$

and δ denotes the summation

$$\delta = \tfrac{3}{35}\phi + \tfrac{9}{425}\phi^2 + \tfrac{11}{1125}\phi^3 + \cdots = \frac{3}{5}\sum_{n=1}^{\infty}\left(\frac{\phi^n}{5^{n-1}n!(10n-3)}\prod_{j=1}^{n}(1 + 5(j-1))\right). \tag{35}$$

The analogous solution for a two-dimensional turbulent lazy plume issuing from a line source is presented in Appendix B.

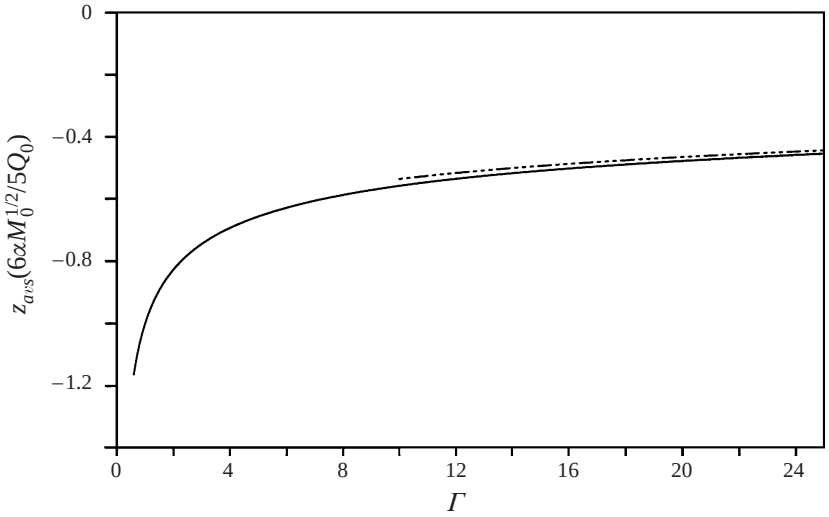

FIGURE 2. The position of the asymptotic virtual source z^*_{avs} (from 34) as a function of the source parameter Γ. $\cdots$—$\cdots$, The large Γ approximation $z^*_{avs} = 0.853\Gamma^{-1/5}$ (36) for $\Gamma > 10$.

The value of z^*_{avs} from (34) is plotted as a function of Γ in figure 2. The solution (34) predicts that, as Γ increases, the displacement z^*_{avs} of the asymptotic virtual source from the actual source decreases. In the limit as $\Gamma \to \infty$, $z^*_{avs} \to 0$ and the location of the asymptotic origin of the lazy plume coincides with the actual source. This limit corresponds to an area source with zero initial volume flux, i.e. a source of buoyancy alone (see (26)). An example of such a source is where a sun patch strongly heats a region of the ground inside a room or building. As $\Gamma \to \infty$, $\phi \to 1$ and the series $\delta(\phi)$ approaches a constant value $\delta(\phi = 1) \approx 0.147$. The approximation $\delta = 0.147$ gives δ accurate to within 5% for $\Gamma > 88$ and the following expression for z_{avs} is therefore recommended

$$z_{avs}\frac{6\alpha M_0^{1/2}}{5Q_0} = 0.853\Gamma^{-1/5} \quad \text{for} \quad \Gamma > 88. \tag{36}$$

The number of terms of (35) required to give $\delta(\phi)$, and hence z_{avs}, to a given level of accuracy increases as the plume becomes increasingly lazy (figure 3).

To compare the magnitude of the asymptotic correction (34) with the jet-length based correction (7), z_{avs}/L_m is plotted as a function of Γ in figure 4. With this scaling, we may readily compare (34) with Morton's integral solutions (12) and (13). Scaled on the jet length (6), our asymptotic correction (34) takes the form

$$\frac{z_{avs}}{L_m} = -2^{3/2}5^{1/2}3^{-1}\Gamma^{3/10}(1-\delta) \approx -2.108\Gamma^{3/10}(1-\delta), \tag{37}$$

and (37) is plotted in figure 4 for $\Gamma > 0.5$ as the solid line. Morton's correction (7) is shown as a cross at $\Gamma = 0$. The (two-step) correction (12) of Morton (1959*a*) is shown as the dashed line for $0 < \Gamma < 1$. With this scaling, the magnitude of z_{avs}/L_m increases as Γ increases. Note, however, that z_{avs} decreases with increasing Γ (figure 2). By expressing Γ as a ratio of the characteristic lengthscales $L_m \sim \hat{M}_0^{3/4}\hat{F}_0^{-1/2}$ and $L_a \sim \hat{Q}_0\hat{M}_0^{-1/2} \sim D$ (from (28)), namely,

$$\Gamma \sim (L_a/L_m)^2, \tag{38}$$

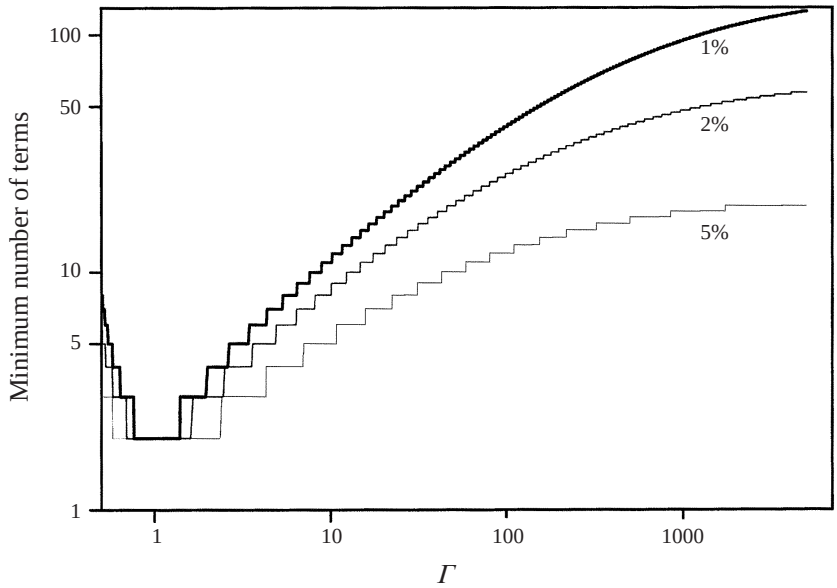

FIGURE 3. The minimum number of terms of (35) required to give δ accurate to within 1%, 2% and 5% *vs.* Γ. Data is plotted for $\Gamma > 0.5$.

it is apparent that for a fixed source diameter D and, hence, fixed L_a, Γ increases as L_m decreases – a decrease in L_m is achieved by reducing $\hat{Q}_0$ and/or g_0'. For a fixed supply rate Q_0 of buoyant fluid, Γ increases as D is increased (see (26)). Thus, Γ increasing may be interpreted as either (i) decreasing the jet length of a plume issuing from a source of constant diameter – in this case z_{avs} decreases with decreasing L_m which is consistent with z_{avs}/L_m increasing as Γ increases (figure 4), or (ii) the source diameter increasing, and hence z_{avs} increasing, for a fixed jet length – again consistent with figure 4. For sufficiently lazy plumes, the jet length will be small compared with the scale of the source and the transition from lazy plume to simple plume as the flow rises above the source will occur over a vertical height which scales on the source diameter. For these sources the jet length is not the appropriate scale.

When $\Gamma = 1$, $\phi = 0$ and $\delta(\phi = 0) = 0$, the area source emits a simple plume and (37) reduces to Morton's (1959*a*) solution (11), or equivalently (34) reduces to

$$z_{avs}\frac{6\alpha M_0^{1/2}}{5Q_0} = 1 \quad \text{for} \quad \Gamma = 1. \tag{39}$$

As $\Gamma \to 0.5$, $\phi \to -1$ and $\delta(\phi = -1) \approx -0.07083$, (37) reduces to $z_{avs}/L_m = -1.834$. Morton's integral solution (12) also yields $z_{avs}/L_m = -1.834$ at $\Gamma = 0.5$. The magnitude of our asymptotic correction and the corrections of Morton for $\Gamma > 0.5$ are identical.

3. Comparison with experiment

In order to test the theoretical predictions developed in § 2, experiments were conducted in the laboratory using saline plumes. The experimental technique we used was first described by Baines (1983) and provides a means of measuring directly the volume flux in a turbulent plume.

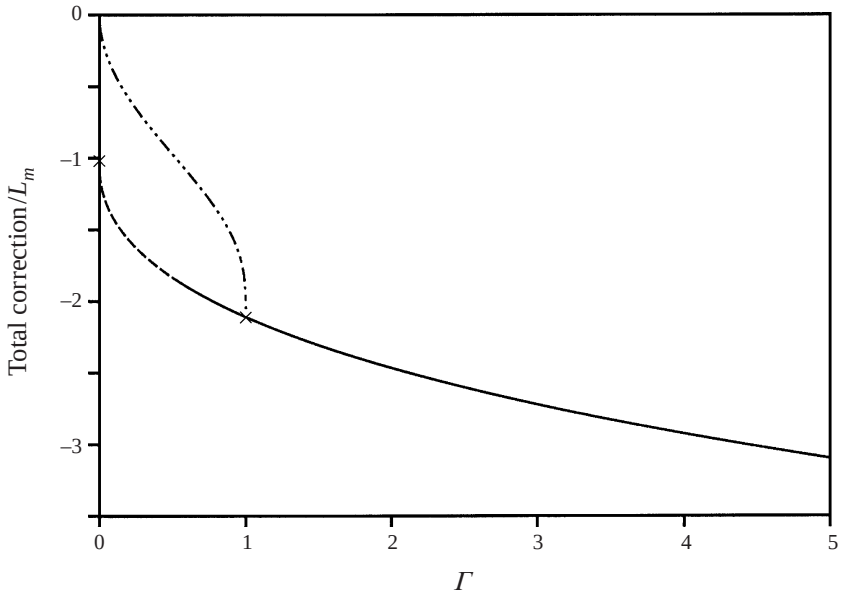

FIGURE 4. The position of the asymptotic virtual source z_{avs}/L_m as a function of Γ. The jet-length based correction (7) of Morton (1959*a*) is shown as the cross at $\Gamma = 0$. Morton's (1959*a*) solution (11) for a simple plume is shown as the cross at $\Gamma = 1$. ——, our asymptotic solution (37) for $\Gamma > 0.5$; — —, the (two-step) solution of Morton (1959*a*) for a forced plume (12) for $0 < \Gamma < 1$; · · —· · ·, the first step.

Experiments were conducted in a clear Perspex tank (of uniform cross-sectional area 64 cm × 64 cm and height 40 cm) filled with fresh water. A sheet of Perspex with cross-sectional area equal to that of the tank was suspended horizontally in the tank a few centimetres below the surface of the water. This sheet was perforated with a number of holes and the plume nozzle, of outlet diameter 5 mm, was located at its centre. Plumes were created by supplying brine to the nozzle, at a constant flow rate, via a constant-head gravity-feed system. In this system, the buoyancy force acts downwards, although for Boussinesq flows this reversal of the direction of the buoyancy force (cf. a thermal plume) does not alter the dynamics of the plume, other than reversing the sense of the fluid motion. The initial flow rate in the plume was measured using an in-line flow meter. The density of the saline supply and of the fresh water ambient was measured using a densitometer, and hence, the buoyancy flux determined. The plume nozzle was designed specifically to produce a turbulent plume and uniform velocity profile at the point of discharge.

The nozzle design, as conceived by Dr Paul Cooper of the University of Wollongong, NSW, Australia, and illustrated schematically in Hunt & Linden (2001), is based on exciting a turbulent flow inside the nozzle prior to the point of discharge. This is achieved by means of an expansion chamber within the nozzle. Fluid fed to the nozzle is forced through a 'pin-hole' (diameter 1 mm) and into a wide expansion chamber (diameter 10 mm). The sharp expansion excites a turbulent flow in the chamber which discharges from the nozzle through the exit opening (diameter 5 mm) after passing through a fine gauge mesh.

Fresh water was supplied to the tank, above the Perspex sheet, at a known constant flow rate. Simultaneously, fluid was drained from the base of the tank at the same flow rate as the fresh water was supplied. Typical supply/drainage flow rates were in the

range of 10–40 $\mathrm{cm^3\,s^{-1}}$ and initial flow rates in the plume were typically 1–2 $\mathrm{cm^3\,s^{-1}}$. The sheet was used to prevent the supply of fresh water from creating disturbances inside the tank.

The turbulent saline plume descended and spread out on reaching the bottom of the tank to form a layer of salt solution. This lower layer increased in depth and density until a steady-state flow was established. The steady flow consisted of a two-layer stratification; a fresh upper layer and a lower layer of salt solution, separated by a horizontal interface. When the interface reached a fixed elevation, a distance z (cm) below the actual source, there was no flow across the interface other than in the plume. Consequently, at the level of the interface the volume flow rate in the plume was identical to the (known) volume flow rate at which the fresh water was supplied to the system. Hence, by measuring the steady height of the interface below the actual source, the volume flow rate in the plume at that distance from the source was deduced. By varying the supply and drainage flow rates, the volume flow rate in the plume was measured at various distances from the actual source.

A dye was added to the saline solution supplied to the plume; this dye coloured the lower salty layer of fluid and allowed the position of the interface to be seen clearly. The experiment was viewed through a video camera which was positioned as far from the tank as possible in order to minimize parallax errors. The images were digitized using the digital image processing system DigImage (Dalziel 1993), and the position of the interface, which corresponded to a particular digitized intensity, was tracked. To be certain of measuring the steady-state interface height, a time series of interface positions was generated on each occasion the supply/drainage flow rate was changed.

In order to evaluate the location (34) of the asymptotic virtual origin, the source parameter Γ characterizing the plume must be determined; this requires measurement of the initial quantities $\hat{Q}_0$, $\hat{F}_0$ and $\hat{M}_0$. The source volume flux $\hat{Q}_0$ was measured to within 0.2 $\mathrm{cm^3\,s^{-1}}$ using an in-line flow meter and the initial buoyancy flux $\hat{F}_0\,(=\hat{Q}_0 g_0')$ was deduced after measuring the reduced gravity g_0' of the saline supply to within $5\times10^{-5}\,\mathrm{cm\,s^{-2}}$ using an Anton Paar density meter. The source momentum flux $\hat{M}_0$, defined as

$$\hat{M}_0 = \int_A w_0^2\,\mathrm{d}A, \tag{40}$$

where w_0 denotes the vertical source velocity, is more challenging to measure accurately as it depends, not only on the initial volume flux, but also on the velocity profile at the source. In turn, this profile depends on the details of the nozzle geometry and source Reynolds number. A technique for the (indirect) measurement of $\hat{M}_0$ is available (see Appendix C) although it depends sensitively on an empirical constant for which there is some considerable uncertainty in the literature regarding the most appropriate value. Owing to this sensitivity and to the design of nozzle used in the experiments (which produced a turbulent flow at the point of discharge) the momentum flux was not determined from experimental measurement but predicted based on the assumption of a uniform velocity profile at the point of discharge of the nozzle, i.e. $\hat{M}_0 = \hat{Q}_0^2/A$.

Results of the experiments are plotted in figures 5 and 6 for source conditions corresponding to $\Gamma = 1.24$, $\Gamma = 2.61$ and $\Gamma = 3.93$. The horizontal axis scale is based on the flow rate scalings of MTT, and the vertical axis scale is the steady interface height z scaled on the source diameter D. The 'raw' experimental data representing interface heights measured above the actual source are shown in figure 5. These measurements have been corrected, using (34), to account for the non-ideal source conditions of the saline plume and are shown in figure 6. The source conditions used

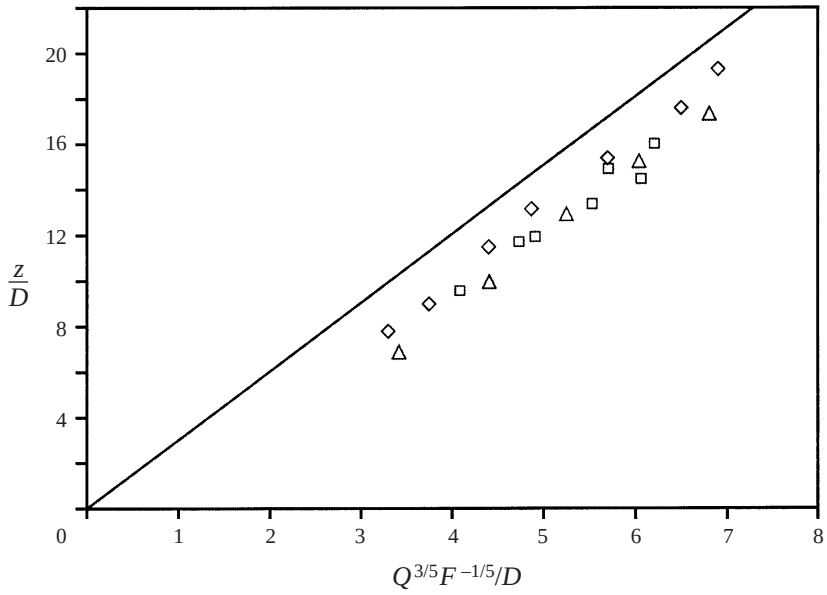

FIGURE 5. Volume flow rate measurements for a turbulent plume uncorrected for the virtual origin of the source. ——, theoretical prediction for $\alpha = 0.09$; □, $\Gamma = 1.24$; △, $\Gamma = 2.61$; ◇, $\Gamma = 3.93$.

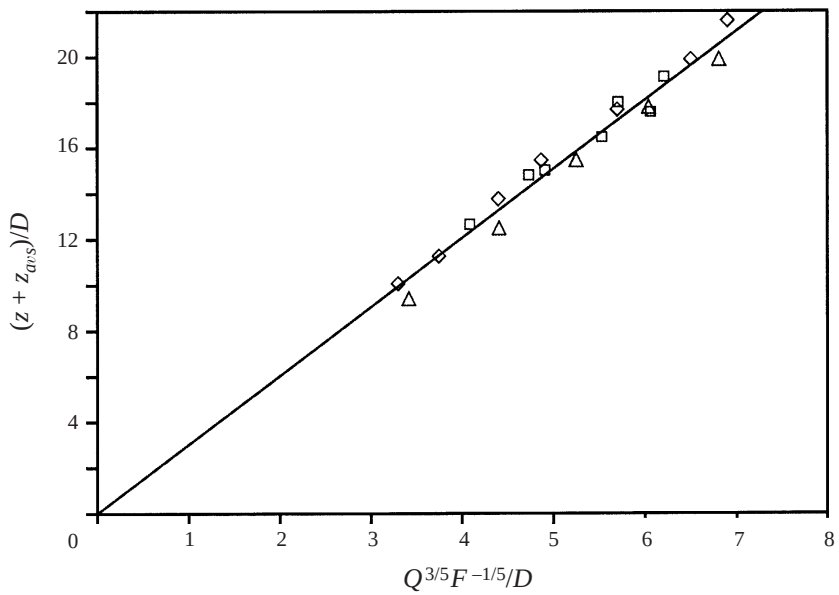

FIGURE 6. Volume flow rate measurements for a turbulent plume corrected for the virtual origin of the source. ——, theoretical prediction for $\alpha = 0.09$; □, $\Gamma = 1.24$; △, $\Gamma = 2.61$; ◇, $\Gamma = 3.93$.

in the experiments are shown in table 1. A sufficient number of terms of the series (35) were summed to ensure that the correction z_{avs} was determined at least to the degree of accuracy with which the interface heights were measured during the experiments. Interface heights were measured to the nearest mm and typically the first five terms of (35) were required to achieve this accuracy. For the range of Γ considered, the sides

Γ	1.24	2.61	3.93
$\hat{Q}_0\,(\mathrm{cm^3\,s^{-1}})$	1.71	1.51	1.09
$g'_0\,(\mathrm{cm\,s^{-2}})$	76.6	126.5	98.2
$\hat{F}_0\,(\mathrm{cm^4\,s^{-3}})$	131.0	191.0	107.0
$\hat{M}_0\,(=\hat{Q}_0^2/A)\,(\mathrm{cm^4\,s^{-2}})$	14.9	11.6	6.06
$L_m = 2^{-5/4}\alpha^{-1/2}\pi^{-1/4}\hat{M}_0^{3/4}\hat{F}_0^{-1/2}\,(\mathrm{cm})$	0.698	0.479	0.393
$L_a = 3^{-1}2^{-3/2}5\alpha^{-1}\pi^{-1/2}\hat{Q}_0\hat{M}_0^{-1/2}\,(\mathrm{cm})$	1.636	1.636	1.646
δ (from (35))	1.746×10^{-2}	6.468×10^{-2}	8.348×10^{-2}
Morton z_{avs}/L_m (from (7))	−1.057	−1.057	−1.057
(*a*) Hunt & Kaye z_{avs}/L_m (from (37))	−2.209	−2.629	−2.913
(*b*) Hunt & Kaye $z_{avs}/D = -3^{-1}2^{-5/2}5\alpha^{-1}\Gamma^{-1/5}(1-\delta)$ (from (34))	−3.081	−2.528	−2.282

TABLE 1. Source conditions of the saline plumes and comparison between resulting jet-length based correction (7) and asymptotic correction (34) of § 2, (*a*) scaled on jet length, and (*b*) scaled on source diameter. $D = 0.5\,\mathrm{cm}$, $\alpha = 0.09$. With L_a as defined above, $\Gamma = 3^2 2^{-3} 5^{-1}(L_a/L_m)^2$.

of the plume were close to parallel at the source. The 'necking' of the plume predicted for $\Gamma > 2.5$ (see (14)) was not visible; however, the small scale of the plume source (5 mm diameter) made flow visualization in the initial development region difficult.

The jet-length based correction (7) which does not account for the finite area of the source, although it is often used to provide an indication of the magnitude of the origin correction, yields $z_{avs} = 0.74$, 0.51 and 0.39 cm for $\Gamma = 1.24$, 2.61 and 3.93, respectively. This compares with $z_{avs} = 1.54$, 1.26 and 1.14 cm, from (34).

By fitting a straight line through the corrected data $(z + z_{avs})/D$ *vs.* $Q^{3/5}F^{-1/5}/D$ a value of α was determined for the experiments. For a point source pure plume, MTT give

$$z = C^{-3/5}Q^{3/5}F^{-1/5}, \tag{41a}$$

where

$$C = \frac{6\alpha}{5}\left(\frac{9\alpha}{5}\right)^{1/3}. \tag{41b}$$

The gradient we expect to see in the data (figure 5) is therefore $C^{-3/5}$, and thus α can be deduced from (41*b*). The slope of the line fitted yields $\alpha = 0.09$ which is within the range quoted in the literature; MTT found that a value of $\alpha = 0.093$ agreed very well with their data while experiments by Baines (1983) yielded $\alpha = 0.074$. The theoretical prediction (41) of MTT with $\alpha = 0.09$ is shown in figures 5 and 6 by the straight line.

On comparing figures 5 and 6 it can be seen that the magnitude of the correction for these experiments was of the order of 1.5 cm or approximately $3D$. The corrected measurements have collapsed onto the theoretical line and there is close agreement, thus confirming the asymptotic virtual origin scaling for lazy plumes.

On the assumption of a uniform velocity profile at the source so that $M_0 = 2^3 Q_0^2/D^2$, the horizontal axis label $Q^{3/5}F^{-1/5}/D$ on figure 5 may be expressed in terms of Γ at $z/D = 0$ as

$$\frac{Q_0^{3/5}F_0^{-1/5}}{D} = \left(\frac{5}{2^{19/2}\alpha}\right)^{1/5}\Gamma^{-1/5}. \tag{42}$$

For a simple plume from an area source, $\Gamma = 1$, and so the theoretical prediction

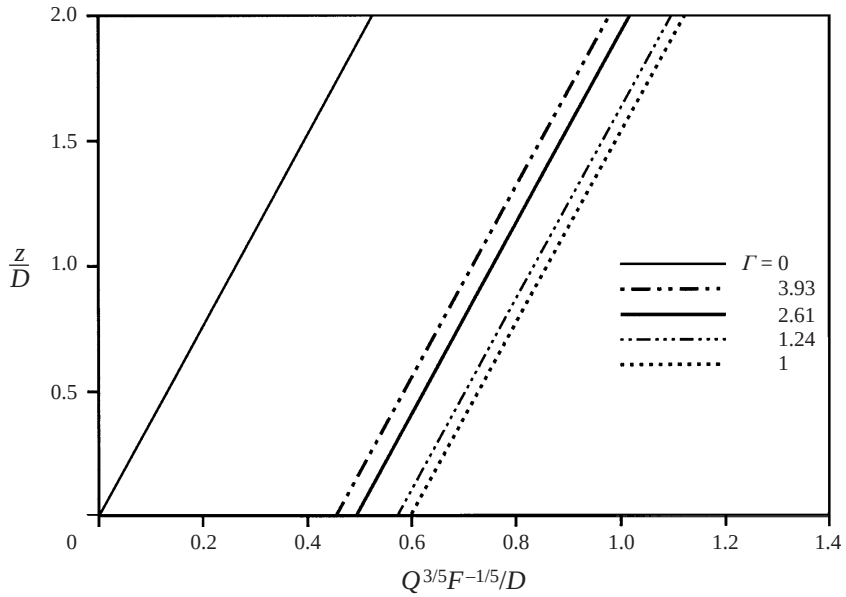

FIGURE 7. z/D *vs.* $Q^{3/5}F^{-1/5}/D$ from (43) for $\Gamma = 0, 1, 1.24, 2.61$ and 3.93. From left to right, the lines correspond to $\Gamma = 0, 3.93, 2.61, 1.24$ and 1, respectively.

of MTT intercepts the horizontal axis at $\lambda = (5/2^{19/2}\alpha)^{1/5} \approx 0.598$ (taking $\alpha = 0.09$). Assuming the gradient $C^{-3/5}$ is appropriate for all source conditions Γ then

$$\frac{z}{D} = C^{-3/5}\left(\frac{Q^{3/5}F^{-1/5}}{D} - \lambda\Gamma^{-1/5}\right), \tag{43}$$

which suggests that the plume appears to originate from a point at

$$\frac{z}{D} = -\lambda C^{-3/5}\Gamma^{-1/5} = -3^{-1}2^{-5/2}5\alpha^{-1}\Gamma^{-1/5}, \tag{44}$$

or, equivalently, at

$$z^* = -\Gamma^{-1/5}. \tag{45}$$

Equation (45) provides a first-order estimate (cf. (34)) of the location of the asymptotic virtual origin. With $\Gamma = 1$, (45) agrees identically with (39) and thus with Morton's simple plume correction, although for $\Gamma < 1$, (45) underestimates, and for $\Gamma > 1$, (45) overestimates the distance between the actual and virtual sources. Figure 7 plots $Q^{3/5}F^{-1/5}/D$ *vs.* z/D from (43), for $\Gamma = 0, 1, 1.24, 2.61$ and 3.93. Correction (34) therefore accounts for the shift between the lines for $\Gamma = 1$ and those for $\Gamma \neq 1$, as opposed to the (greater) shift between lines representing the point source solution $\Gamma = 0$ and solutions for $\Gamma \neq 1$.

4. Conclusions

We have considered the location of the asymptotic virtual origin of forced buoyant plumes generated by general extended sources (F_0, M_0, Q_0) of non-zero initial buoyancy, momentum and volume fluxes. Buoyant plumes are characterized by the source parameter Γ and we present an explicit formulation for calculating the asymptotic virtual origin for source conditions in the range $\Gamma > 1/2$. This correction encompasses

a wide range of typical source conditions which include: (i) forced plumes (with an excess of initial momentum flux compared with the equivalent pure plume) in the range $1/2 < \Gamma < 1$; (ii) pure plumes, i.e. plumes with source conditions giving $\Gamma = 1$; and (iii) lazy plumes (with a deficiency of initial momentum flux when compared with the equivalent pure plume) for $\Gamma > 1$. We have shown that plumes arising from these sources are equivalent to point source pure plumes $(F_0, 0, 0)$, of buoyancy only, located at an asymptotic virtual source located behind the actual source at $z = 0$.

For $\Gamma > 1/2$, the appropriate lengthscale for the adjustment of a turbulent plume to that of a point source pure plume is the source radius and comparisons made between the predicted location of the asymptotic virtual origin and its location deduced from measurements of volume flow rate in turbulent saline plumes for $\Gamma > 1$ show close agreement, supporting the scalings used in the analysis.

It is questionable whether the standard entrainment assumption of MTT, namely, that the entrainment velocity is a constant fraction α of the vertical velocity, is appropriate near the source of plumes with source conditions yielding $\Gamma \gg 1$. In the region of the plume undergoing contraction, vertical velocities are relatively low and the flow is unlikely to be fully turbulent. An investigation of the rate of entrainment close to the source for $\Gamma \gg 1$ is currently under progress.

G. R. H. would like to acknowledge the financial support of the EPSRC and the Building Research Establishment through the Department of the Environment's Energy Related Environmental Issues (EnREI) in Buildings programme. N. G. K. would like to acknowledge the financial support of the Commonwealth Scholarship Commission and the British Council. The authors would also like to thank Paul Linden for the many useful discussions and his comments made during the preparation of this work. We also acknowledge the comments of an anonymous referee.

Appendix A

Although not stated explicitly in Morton (1959*a*), the constant -1.057 in (7) is obtained after summing the series

$$\delta_m = \sum_{n=1}^{\infty} \left(\frac{1}{2^{n-1} n!(3-10n)} \prod_{m=1}^{n} [1 + 2(m-1)] \right) \approx -0.3324 \tag{A 1}$$

which enters the expression for the virtual source as follows

$$\frac{z_v}{L_m} = -2^{1/2} 5^{1/2} (\tfrac{2}{3} + \delta_m) \approx -1.057. \tag{A 2}$$

The series represents an approximation to the integral

$$z = 2^{1/2} 5^{1/2} \int_1^v (v^5 - 1)^{-1/2} v^3 \, \mathrm{d}v, \tag{A 3}$$

where $v = (M/M_0)^{1/2}$, such that

$$\frac{z}{2^{1/2} 5^{1/2}} \approx \tfrac{2}{3} v^{3/2} + O(v^{-7/2}) - \left[\tfrac{2}{3} + \delta_m \right]. \tag{A 4}$$

Appendix B

Adopting the standard entrainment assumption (Morton *et al.* 1956) the flow above a two-dimensional turbulent line plume in an unstratified environment and in the

Boussinesq limit may be described by the system of conservation equations

$$\mathrm{d}\hat{Q}_L/\mathrm{d}z = 2a\alpha\hat{M}_L/\hat{Q}_L, \tag{B 1}$$

$$\mathrm{d}\hat{M}_L/\mathrm{d}z = \hat{Q}_L\hat{B}_L/\hat{M}_L, \tag{B 2}$$

$$\mathrm{d}\hat{B}_L/\mathrm{d}z = 0, \tag{B 3}$$

where the subscript L denotes 'per unit length' and $a = \sqrt{2}$ for Gaussian profiles. Here, B, Q and M denote the actual fluxes. Non-dimensionalized on the source conditions (B 1)–(B 2) reduced to

$$\mathrm{d}q_L/\mathrm{d}z^* = m_L/q_L, \tag{B 4}$$

$$\mathrm{d}m_L/\mathrm{d}z^* = \Gamma_L q_L/m_L, \tag{B 5}$$

where $q_L = \hat{Q}_L/\hat{Q}_{L0}$, $m_L = \hat{M}_L/\hat{M}_{L0}$, $z^* = 2a\alpha(\hat{M}_{L0}/\hat{Q}_{L0}^2)z$ and the source parameter

$$\Gamma_L = \frac{1}{2a\alpha}\frac{Q_{L0}^3 B_{L0}}{M_{L0}^3}. \tag{B 6}$$

Following an analysis similar to that presented in § 2 we find that

$$\Gamma_L^{1/3} z^* = \int_1^q q(q^3 - \phi_L)^{-1/3}\mathrm{d}q, \tag{B 7}$$

where

$$\phi_L = \frac{\Gamma_L - 1}{\Gamma_L}. \tag{B 8}$$

It may then be shown that the non-idealized two-dimensional line plume (B_{L0}, M_{L0}, Q_{L0}) may be replaced by the point source pure plume $(B_{L0}, 0, 0)$ located a distance

$$\frac{z_{avs}}{(Q_{L0}^2/2a\alpha M_{L0})} = \frac{1-\delta_L}{\Gamma_L^{1/3}}, \tag{B 9}$$

behind the actual source, where δ_L denotes the series

$$\delta_L = \sum_{n=1}^{\infty}\left(\frac{\phi_L^n}{n!(3n-1)}\prod_{j=1}^{n}\left(\frac{1+3(j-1)}{3}\right)\right). \tag{B 10}$$

This correction is valid providing $\Gamma_L > 0.5$.

Appendix C

For a parabolic velocity profile (laminar flow) at the nozzle exit

$$\hat{M}_0 = \frac{2}{\sqrt{3}}\frac{\hat{Q}_0^2}{A}, \tag{C 1}$$

whereas for a uniform velocity profile (turbulent outflow)

$$\hat{M}_0 = \hat{Q}_0^2/A, \tag{C 2}$$

i.e. $\hat{M}_0$ is approximately 15% larger for a laminar outflow, and these extremes of outflow profiles lead to differences of approximately 30% in the resulting values of $\Gamma (\sim \hat{M}_0^{-5/2})$.

Baines, Turner & Campbell (1990) propose a technique for the (indirect) measurement of the source momentum flux $\hat{M}_0$ based on a variation of the original 'filling box' experiment of Baines & Turner (1969). A weakly buoyant jet, rather than a highly buoyant plume (cf. Baines & Turner 1969), is used as the source in the filling box and the position of the first 'front' tracked in time. The method, as outlined below and adopted, for example, by Bloomfield & Kerr (1998), relies on the initial momentum flux $\hat{M}_0$ being conserved. The flow from the source is therefore required to be essentially jet-like over the entire height H of the box (this requires that the jet length $\sim \hat{M}_0^{3/4}/\hat{F}_0^{1/2}$ be significantly larger than H) although a small density contrast is necessary to establish the front. In practice, even for source conditions giving $\hat{M}_0^{3/4}/\hat{F}_0^{1/2} \approx H$, establishing a saline front is difficult owing to considerable mixing which occurs when the jet-like flow collides with the base of the container and, in addition, owing to the subsequent 'overturning' motion as the resulting outflow collides with the sidewalls of the container and is forced upwards before being entrained into the jet. The true 'filling box' behaviour with a horizontal front as described by Baines & Turner (1969) was typically not established.

The rate of change in the vertical position z_0 of the front from the source is dependent upon the volume flow rate $\hat{Q}(z_0)$ in the weakly buoyant jet at the height of the front and the cross-sectional area S of the box:

$$\mathrm{d}z_0/\mathrm{d}t = \hat{Q}(z_0)/S. \tag{C 3}$$

Providing the initial momentum flux $\hat{M}_0$ of the source is conserved, then the volume flow rate at the front is of the form

$$\hat{Q} = C_j \hat{M}_0^{1/2}(z + z_{vj})|_{z=z_0}, \tag{C 4}$$

(see Fischer *et al.* 1979), where z_{vj} denotes the virtual origin of the jet and C_j, an empirical constant. Following Baines & Turner (1969) we assume that the first front forms instantaneously at the ceiling of the box, i.e. at time $t = 0$, $z_0 = H$. Combining (B 1) and (B 2) and integrating gives

$$\ln\left(\frac{z_0 + z_{vj}}{H}\right) = C_j \frac{\hat{M}_0^{1/2}}{S} t. \tag{C 5}$$

Plotting the data from experiment in the form of $\ln((z_0 + z_{vj})/H)$ against time should yield a straight line with a gradient of $C_j \hat{M}_0^{1/2}/S$ for the appropriate value of z_{vj} (which may be deduced using the iterative method of Baines & Turner 1969) providing the flow is jet-like and the box fills in a classical filling box fashion. By fitting a straight line to the data, the gradient may be measured and, hence, the initial momentum flux determined. This method is sensitive to the gradient of the fit as $\hat{M}_0 \sim \text{gradient}^2$. Furthermore, considerable variability in the value of the coefficient C_j has been recorded in the literature: $C_j = 0.25$ (Fischer *et al.* 1979), 0.282 (Ricou & Spalding 1961) and 0.404 (Schlichting 1968). This variation leads to a high degree of uncertainty regarding the value of $\hat{M}_0$ deduced. For example, if instead of taking $C_j = 0.25$ (Fischer *et al.* 1979) we take $C_j = 0.282$ (Ricou & Spalding 1961), $\hat{M}_0$ increases by over 27%. This increase is almost double the difference in the source momentum flux between laminar and turbulent flows (see (C 1) and (C 2)).

Owing to the design of the nozzles used in the lazy plume experiments reported herein, the source momentum flux was not determined experimentally but rather the velocity profile was taken to be uniform so that $\hat{M}_0 = \hat{Q}_0^2/A$.

REFERENCES

Baines, W. D. 1983 A technique for the direct measurement of volume flux of a plume. *J. Fluid Mech.* **132**, 247–256.

Baines, W. D. & Turner, J. S. 1969 Turbulent buoyant convection from a source in a confined region. *J. Fluid Mech.* **37**, 51–80.

Baines, W. D., Turner, J. S. & Campbell, I. H. 1990 Turbulent fountains in an open chamber. *J. Fluid Mech.* **212**, 557–592.

Baker, C. B., George, W. K. & Taulbee, D. B. 1980 An analysis of the axisymmetric turbulent buoyant jet. *Proc. 7th Intl Heat Transfer Conf. Munich*, vol. 2, pp. 383–388.

Batchelor, G. K. 1954 Heat convection and buoyancy effects in fluids. *Q. J. R. Met. Soc.* **80**, 339–358.

Bloomfield, L. J. & Kerr, R. C. 1998 Turbulent fountains in a stratified fluid. *J. Fluid Mech.* **385**, 335–356.

Caulfield, C. P. 1991 Stratification and buoyancy in geophysical flows. PhD thesis, University of Cambridge, UK.

Caulfield, C. P. & Woods, A. W. 1995 Plumes with non-monotonic mixing behaviour. *Geophys. Astrophys. Fluid Dyn.* **79**, 173–199.

Dalziel, S. B. 1993 Rayleigh–Taylor instability: experiments with image analysis. *Dyn. Atmos. Oceans* **20**, 127–153.

Fischer, H. B., List, E. J., Koh, R. C. Y., Imberger, J. & Brooks, N. H. 1979 *Mixing in Inland and Coastal Waters.* Academic. ISBN 0-12-258150-4.

George, W. K. Jr., Alpert, R. L. & Tamanini, F. 1977 Turbulence measurements in an axisymmetric buoyant plume. *Intl J. Heat Mass Transfer* **20**, 1145–1154.

Hunt, G. R. & Linden, P. F. 2001 Steady-state flows in an enclosure ventilated by buoyancy forces assisted by wind. *J. Fluid Mech.* **426**, 355–386.

Kotsovinos, N. E. & List, E. J. 1977 Plane turbulent buoyant jets. Part 1. Integral properties. *J. Fluid Mech.* **81**, 25–44.

List, E. J. 1982 Turbulent jets and plumes. *Ann. Rev. Fluid Mech.* **14**, 189–212.

Morton, B. R. 1959*a* Forced plumes. *J. Fluid Mech.* **5**, 151–163.

Morton, B. R. 1959*b* The ascent of turbulent forced plumes in a calm atmosphere. *Intl J. Air Poll.* **1**, 184–197.

Morton, B. R. & Middleton, J. 1973 Scale diagrams for forced plumes. *J. Fluid Mech.* **58**, 165–176.

Morton, B. R., Taylor, G. I. & Turner, J. S. 1956 Turbulent gravitational convection from maintained and instantaneous sources. *Proc. R. Soc. Lond.* **234**, 1–23.

Nakagome, H. & Hirita, M. 1977 The structure of turbulent diffusion in an axisymmetrical thermal plume. In *Proc. 1976 ICHMT Seminar on Turbulent Buoyant Convection*, pp. 361–392. Hemisphere.

Papanicolaou, P. N. & List, E. J. 1988 Investigation of round turbulent buoyant jets. *J. Fluid Mech.* **195**, 341–391.

Ricoh, F. P. & Spalding, D. B. 1961 Measurements of entrainment by axisymmetrical turbulent jets. *J. Fluid Mech.* **11**, 21–32.

Rouse, H., Yih, C. S. & Humphreys, H. W. 1952 Gravitational convection from a boundary source. *Tellus* **4**, 201–210.

Schlicting, H. 1968 *Boundary-Layer Theory*, 6th edn. McGraw-Hill.

Schmidt, W. 1941 Turbulente ausbreitung eines stromes erhizter luft. *Z. Angew. Math. Mech.* **21**, 265–278.

Shabbir, A. & George, W. K. 1994 Experiments on a round turbulent buoyant plume. *J. Fluid Mech.* **275**, 1–32.

Turner, J. S. 1966 Jets and plumes with negative and reversing buoyancy. *J. Fluid Mech.* **26**, 779–792.

Turner, J. S. 1986 Turbulent entrainment: the development of the entrainment assumption. *J. Fluid Mech.* **173**, 431–472.